From Spin Glass to Quantum Spin Liquid Ground States in Molybdate Pyrochlores

L. Clark,[1] G. J. Nilsen,[2] E. Kermarrec,[1] G. Ehlers,[3] K. S. Knight,[4] A. Harrison,[5,6] J. P. Attfield,[5] and B. D. Gaulin[1,7,8]
[1]Department of Physics and Astronomy, McMaster University, Hamilton, Ontario L8S 4M1, Canada
[2]Institute Laue-Langevin, 6 Rue Jules Horowitz, 38042 Grenoble, France
[3]Neutron Scattering Science Division, Oak Ridge National Laboratory, Oak Ridge, Tennessee 37831, USA
[4]ISIS Facility, Rutherford Appleton Laboratory, Didcot, Oxfordshire OX11 0QX, United Kingdom
[5]CSEC and School of Chemistry, University of Edinburgh, Mayfield Road, Edinburgh EH9 3JZ, United Kingdom
[6]Diamond Light Source, Harwell Science and Innovation Campus, Didcot, Oxfordshire OX11 0QX, United Kingdom
[7]Brockhouse Institute for Materials Research, Hamilton, Ontario L8S 4M1, Canada
[8]Canadian Institute for Advanced Research, 180 Dundas Street West, Toronto, Ontario M5G 1Z8, Canada
(Received 5 May 2014; revised manuscript received 18 August 2014; published 8 September 2014)

We present new magnetic heat capacity and neutron scattering results for two magnetically frustrated molybdate pyrochlores: $S = 1$ oxide $Lu_2Mo_2O_7$ and $S = \frac{1}{2}$ oxynitride $Lu_2Mo_2O_5N_2$. $Lu_2Mo_2O_7$ undergoes a transition to an unconventional spin glass ground state at $T_f \sim 16$ K. However, the preparation of the corresponding oxynitride tunes the nature of the ground state from spin glass to quantum spin liquid. The comparison of the static and dynamic spin correlations within the oxide and oxynitride phases presented here reveals the crucial role played by quantum fluctuations in the selection of a ground state. Furthermore, we estimate an upper limit for a gap in the spin excitation spectrum of the quantum spin liquid state of the oxynitride of $\Delta \sim 0.05$ meV or $\Delta/|\theta| \sim 0.004$, in units of its antiferromagnetic Weiss constant $\theta \sim -121$ K.

DOI: 10.1103/PhysRevLett.113.117201 PACS numbers: 75.10.Kt, 75.40.Cx, 75.50.Lk

Geometric magnetic frustration results when the arrangement of magnetic moments on an ordered lattice prevents the satisfaction of magnetic exchange interactions [1]. This can generate a macroscopic ground state degeneracy, whereby spins on the vertices of the frustrated lattice fluctuate within a manifold of nonordered states. In materials with both strong geometric frustration and small ($S = \frac{1}{2}$) magnetic moments, quantum fluctuations can induce a quantum spin liquid (QSL) ground state [2,3]. There are now several promising materials that host this state in two-dimensional frustrated lattices [4–8]. However, examples of three-dimensional QSL candidates, such as a $S = \frac{1}{2}$ pyrochlore antiferromagnet that possesses a frustrated magnetic lattice of corner sharing tetrahedra, remain scarce [9]. There is some uncertainty regarding the exact nature of the ground state of a $S = \frac{1}{2}$ pyrochlore antiferromagnet [10–12] and the synthesis and study of such materials remain important tasks [13].

Frustration in rare earth molybdate pyrochlores, $R_2Mo_2O_7$, arises from exchange interactions between Mo^{4+} $4d^2$ $S = 1$ spins residing on a network of vertex sharing tetrahedra. Among the phenomena observed in these materials [14], the spin glass state in the apparently disorder-free $Y_2Mo_2O_7$ is of particular interest [15–19]. As this state—a spin glass in the absence of any significant chemical or bond disorder—is very unusual, its realization in a similarly simple material may be revealing. $Lu_2Mo_2O_7$ is a sister compound to $Y_2Mo_2O_7$ and exhibits strong antiferromagnetic exchange, with the Weiss constant $\theta = -160$ K, as well as a spin freezing transition at $T_f \sim 16$ K [20]. These parameters are remarkably close to $Y_2Mo_2O_7$ with $\theta \sim -200$ K and $T_f \sim 22$ K.

A group of materials related to the $R_2Mo_2O_7$ pyrochlores are the corresponding oxynitride phases. Oxynitrides are mixed anion materials that are often prepared by topochemical nitridation of an oxide precursor. As such, oxynitrides of $R_2Mo_2O_7$ retain the cubic pyrochlore structure. The incorporation of the nitride (N^{3-}) anion into the oxide (O^{2-}) framework is accompanied by oxidation of the molybdenum cations to maintain charge neutrality. Oxynitrides of composition $R_2Mo_2O_5N_2$ possess $S = \frac{1}{2}$ spins from Mo^{5+} $4d^1$. Therefore, they are the first potential realization of a d^1 Heisenberg pyrochlore antiferromagnet and are excellent candidates for the study of QSL phenomena [21]. Here we present a comparison of low temperature heat capacity and neutron scattering studies of $Lu_2Mo_2O_7$ and $Lu_2Mo_2O_5N_2$.

Polycrystalline $Lu_2Mo_2O_7$ was synthesized as described elsewhere [20]. An oxynitride phase with a composition close to the ideal $S = \frac{1}{2}$ stoichiometry was prepared by thermal ammonolysis of a $Lu_2Mo_2O_7$ precursor [22]. The oxynitride system adopts the $Fd\bar{3}m$ pyrochlore structure with oxide and nitride anions disordered over the two available anion sites (see Fig. S1 in the Supplemental Material [22]). Magnetic susceptibility of the oxynitride (see Fig. S2 [22]) reveals an absence of long range order or spin freezing down to 2 K despite $\theta = -121(1)$ K. $\mu_{\text{eff}} = 1.11(1)\mu_B$ per Mo cation reflects the oxidation of Mo^{4+} to Mo^{5+}. The 64% reduction of the observed μ_{eff} from the expected spin-only value for $S = \frac{1}{2}$ is consistent with the

 © 2014 American Physical Society

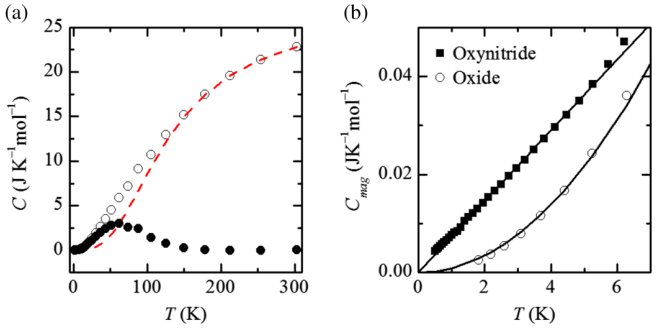

FIG. 1 (color online). (a) Total heat capacity C of $Lu_2Mo_2O_7$ (open circles) with the estimated lattice (dashed line) and magnetic C_{mag} (closed circles) contributions. (b) The magnetic heat capacities of the oxide and oxynitride phases.

67% reduction from the expected $S = 1$ spin-only moment displayed by $Lu_2Mo_2O_7$ [20]. This suggests that spin-orbit coupling is significant in both of these $4d$ systems.

Heat capacity of $Lu_2Mo_2O_7$ was measured on a 9.0 mg pellet in a Quantum Design physical property measurement system (PPMS). The high temperature data were modeled by the Debye equation [Fig. 1(a)] which gave a Debye temperature $\theta_D = 540$ K. Upon subtraction of this estimated lattice contribution, a broad hump centered ~50 K is observed in the magnetic heat capacity C_{mag}, typical of a spin glass system. Heat capacity of the oxynitride was measured on a 8.9 mg sample over 0.5–30 K using a ^{3}He insert. Given the similar structure and formula weight of the oxide and oxynitride phases, the lattice contribution estimated for $Lu_2Mo_2O_7$ was also used to extract the magnetic heat capacity of the oxynitride. A comparison of the low temperature magnetic heat capacities of the oxide and oxynitride are shown in Fig. 1(b). The temperature dependencies are markedly different with $C_{\mathrm{mag}} \propto T^2$ for the oxide and $C_{\mathrm{mag}} \propto T$ for the oxynitride.

Diffuse magnetic neutron diffraction was measured for both pyrochlores on the $D7$ Spectrometer at the Institut Laue-Langevin [28]. xyz polarization analysis was used to separate the components of total neutron scattering [29,30]. Data were collected with an incident wavelength $\lambda = 4.8$ Å, at which final energies are integrated up to $E \sim 3.5$ meV. A detailed experimental account is given in the Supplemental Material [22]. Figure 2 shows the magnetic scattering cross sections $(d\sigma/d\Omega)_{\mathrm{mag}}$ of the oxide and oxynitride at 1.5 K, well below $T_f \sim 16$ K. The magnetic diffuse scattering from the oxide displays a broad peak centered around 0.6 Å^{-1} that indicates the presence of static short ranged molybdenum spin correlations, which were modeled by [31],

$$\left(\frac{d\sigma}{d\Omega}\right)_{\mathrm{mag}} = \frac{2}{3}(\gamma_n r_0)^2 \left(\frac{1}{2} g F(Q)\right)^2 \times \left(S(S+1) + \sum_i Z_i \langle \mathbf{S}_0 \cdot \mathbf{S}_i \rangle \frac{\sin Q r_i}{Q r_i}\right), \quad (1)$$

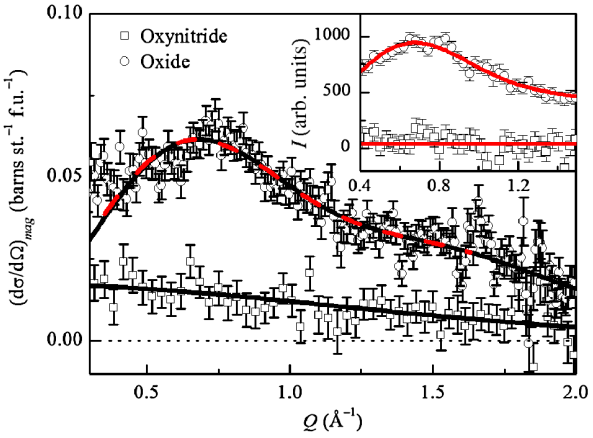

FIG. 2 (color online). The magnetic scattering cross sections of the both samples at 1.5 K. The solid lines are fits to the data. The inset shows the elastic magnetic scattering measured on CNCS at 1.5 K. A scaled version of the fit of Eq. (1) to the CNCS oxide data is shown on top of the $D7$ data (dashed line).

where $\langle \mathbf{S}_0 \cdot \mathbf{S}_i \rangle$ gives the correlation between a spin and its Z_i nearest neighbors at a distance r_i. γ_n, r_0, and g take their usual definitions and $F(Q)$ is the molybdenum form factor [32]. The best fit to the data (Fig. 2) was obtained by allowing for nearest-($r_1 = 3.581$ Å, $Z_1 = 6$) and next-nearest-neighbor ($r_2 = 6.203$ Å, $Z_2 = 12$) correlations $\langle \mathbf{S}_0 \cdot \mathbf{S}_1 \rangle = -0.029(6)$ and $\langle \mathbf{S}_0 \cdot \mathbf{S}_2 \rangle = -0.056(7)$, respectively. In contrast, the magnetic diffuse scattering of the oxynitride at 1.5 K is much weaker than that of the oxide and appears to follow $F(Q)^2$. These data were thus modeled using Eq. (1) with $\langle \mathbf{S}_0 \cdot \mathbf{S}_i \rangle = 0$ for all i [33]. The fit is shown as the solid line against the oxynitride data in Fig. 2. The effective magnetic moment extracted from the fit to the data, $0.11(1)\mu_B$, corresponds to only 6% of the expected $S = \frac{1}{2}$ spin-only value, suggesting that most of the scattering from the oxynitride is inelastic and thus outside the energy range over which $D7$ integrates energy [34].

To probe their full static and dynamic behavior, both samples were studied on the Cold Neutron Chopper Spectrometer (CNCS) [35] at the Spallation Neutron Source of the Oak Ridge National Laboratory. Measurements were performed on cooling to 1.5 K with an incident neutron energy $E_i = 3.3$ meV. The inset of Fig. 2 shows the elastic scattering from the oxide and oxynitride at 1.5 K, obtained by integrating the inelastic spectra over the energy of the elastic line, $E = [-0.1, 0.1]$ meV. A broad peak at low Q is observed for the oxide, which can again be modeled by Eq. (1). To confirm the consistency of the analyses of the CNCS and $D7$ data sets, a scaled version of the fit to the CNCS data is plotted with the $D7$ fit in the main panel of Fig. 2; agreement is excellent. Remarkably, the scattering collected for the oxynitride at 1.5 K within the narrowly defined elastic window on the CNCS is consistent with *no elastic magnetic scattering*, as shown in the inset to Fig. 2.

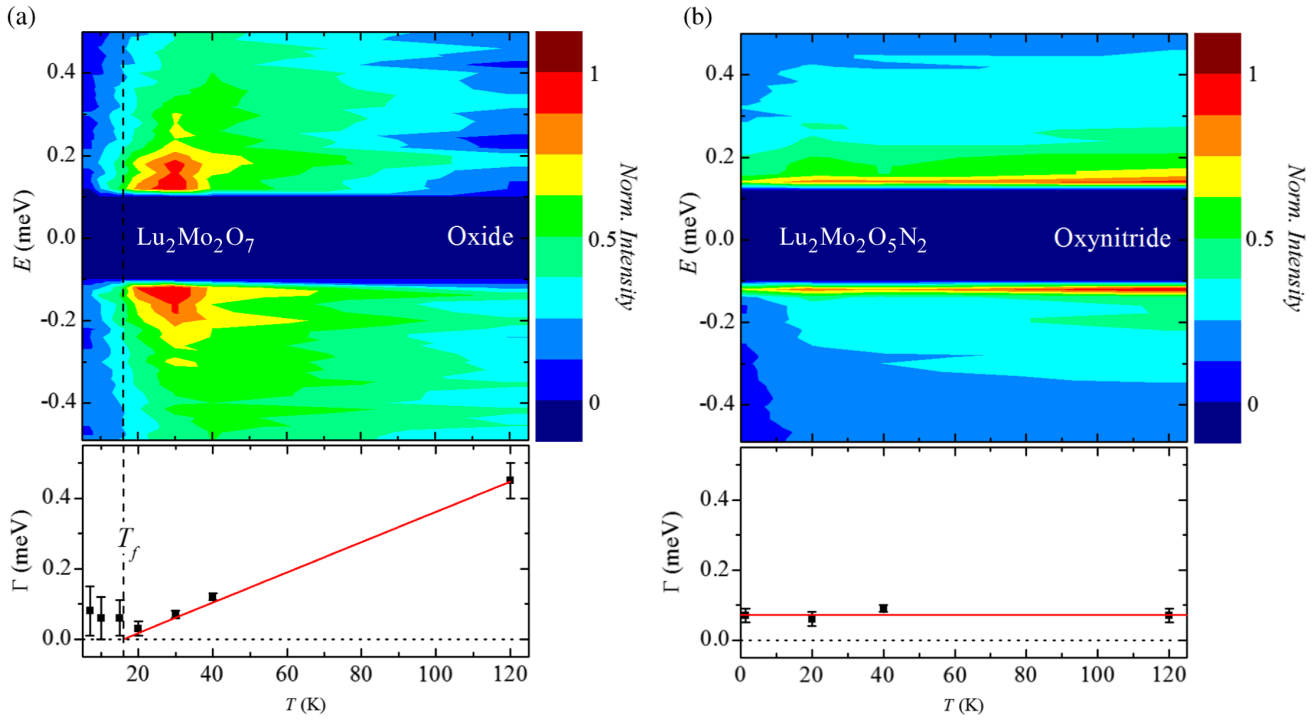

FIG. 3 (color online). The temperature dependence of background subtracted, normalized inelastic neutron scattering ($Q = [0.5, 2.0]$ Å^{-1}) (top) and the energy width of the inelastic spectra, Γ, (bottom) for the (a) oxide and (b) oxynitride, respectively.

The temperature dependencies of the background corrected, normalized, and Q-integrated ($Q = [0.5, 2.0]$ Å^{-1}) inelastic scattering for the oxide and oxynitride are shown in the top panels of Figs. 3(a) and 3(b), respectively. The oxide [Fig. 3(a)] presents a broad spectrum at $T > 50$ K, well above the spin freezing transition. Upon cooling, low energy spin fluctuations develop. The transition is clearly marked by a collapse of inelastic scattering intensity into the elastic line as static short range spin correlations build up. The inelastic scattering data were fitted to the general form of the scattering function [17],

$$S(E) = \frac{1}{\pi}\chi''(E)[1 + n(E)], \tag{2}$$

where $n(E)$ is the Bose-Einstein thermal population factor and χ'' is the imaginary part of the dynamic susceptibility. A good description of the data was obtained with

$$\chi''(E) = \chi_0 \arctan\left(\frac{E}{\Gamma}\right), \tag{3}$$

where Γ is related to the energy width of the inelastic spectrum. Representative fits to the oxynitride data are shown in Fig. 4. The bottom panel of Fig. 3(a) shows the temperature dependence of Γ for the oxide, which goes to zero at or near $T_f \sim 16$ K, consistent with spin glass freezing. The overall dynamic behavior of $Lu_2Mo_2O_7$ is thus very similar to that of its sister "disorder free" spin glass pyrochlore $Y_2Mo_2O_7$ [17]. Again in rather stark contrast, the oxynitride displays a temperature-independent energy width of $\Gamma \sim 0.08$ meV, consistent with that of $Lu_2Mo_2O_7$ near 30 K, almost twice T_f [Fig. 3(b)]. Therefore the temperature dependence observed in $S(E)$ for the oxynitride originates entirely from the Bose-Einstein factor in Eq. (2).

Figure 5 compares the inelastic scattering integrated over $Q = [0.5, 2.0]$ Å^{-1} from both samples at 1.5 K. Given that the inelastic scattering from $Lu_2Mo_2O_7$ is strongly suppressed below T_f, the scattering from the oxide at 1.5 K

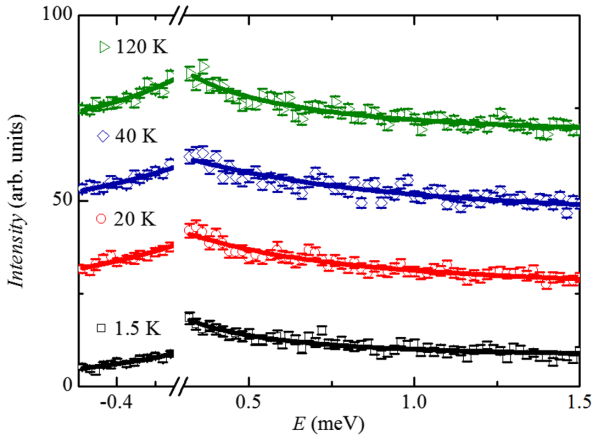

FIG. 4 (color online). Offset E cuts ($Q = [0.5, 2.0]$ Å^{-1}) for the oxynitride sample at various temperatures with fits (solid lines) of Eq. (2) to the data.

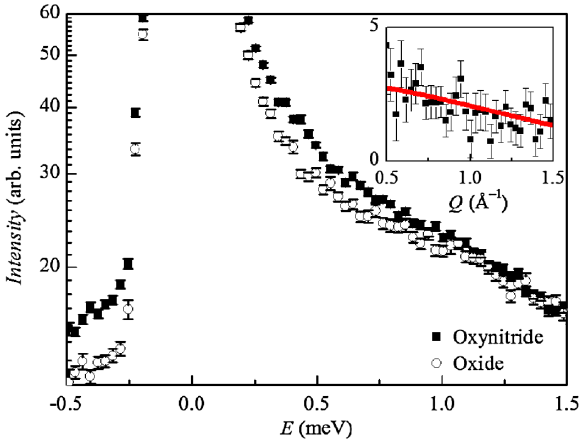

FIG. 5 (color online). E cuts of the oxide and oxynitride neutron scattering spectra at 1.5 K ($Q = [0.5, 2.0]$ Å^{-1}). Inset: Q dependence of the background subtracted inelastic scattering from the oxynitride sample at the same temperature, to which an $F(Q)^2$ form was fitted (solid line).

is a good measure of the background. The oxynitride sample clearly shows an enhanced inelastic signal on either side of the elastic line. The persistence of inelastic scattering, particularly on the neutron energy gain side where the incident neutron destroys a spin fluctuation, directly demonstrates that the oxynitride remains strongly fluctuating at $1.5 \sim |\theta|/100$ K. By subtracting the 1.5 K oxide data from the oxynitride data and integrating in energy ($E = [0.2, 1.5]$ meV) the Q dependence of the inelastic scattering from the oxynitride is obtained (see Fig. 5, inset). The form of this inelastic scattering reveals the nature of dynamical spin correlations within the oxynitride. The Q dependence is well described by the magnetic form factor, $F(Q)^2$. The inelastic magnetic scattering from $Lu_2Mo_2O_5N_2$ strongly suggests a gapless QSL state at 1.5 K, with few or no structured spatial correlations between the $S = \frac{1}{2}$ spins.

Our study of $Lu_2Mo_2O_7$ and $Lu_2Mo_2O_5N_2$ presents both interesting similarities and contrasts. They share the same structure and their magnetic interactions are antiferromagnetic and of similar strength. Yet the $S = 1$ $Lu_2Mo_2O_7$ undergoes a freezing transition at $T_f \sim 16$ K, while the $S = \frac{1}{2}$ $Lu_2Mo_2O_5N_2$ remains in a dynamic state to temperatures $\sim|\theta|/100$. Even though structural disorder and magnetic frustration often lead to spin freezing, $Lu_2Mo_2O_5N_2$ does *not* find a frozen ground state despite O/N disorder, unlike both $Lu_2Mo_2O_7$ and $Y_2Mo_2O_7$. These contrasts are clearly expressed in the low temperature magnetic heat capacities, where $C_{\rm mag} \propto T^2$ for the oxides and $C_{\rm mag} \propto T$ for the oxynitride. The T^2 dependence may arise from the coupling between spin and orbital degrees of freedom in $Y_2Mo_2O_7$ [19] and this spin-orbital frustration was also shown to be an important parameter in the spin glass ground state of $R_2Mo_2O_7$ in recent density functional theory calculations [36]. Linear temperature dependencies have been observed in a number of QSL candidate materials [7,37,38]. The pronounced $C_{\rm mag} = \gamma T$ form, where γ is the Sommerfield coefficient, in spite of insulating behavior is argued to arise from the presence of a spinon Fermi surface [39]. There are examples of frustrated systems in which doping results in a significant enhancement of the linear γT term of heat capacity, such as $Yb_4As_{3-x}P_x$ [40] and $Y_{1-x}Sc_xMn_2$ [41]. In the latter, Sc doping of only $x = 0.03$ is sufficient to break the antiferromagnetic order observed in the parent $YnMn_2$ and induces a tenfold increase in the magnitude of γ [42]. For $Yb_4As_{3-x}P_x$, doping with phosphorous increases γ by a factor of two (for $x = 0.3$), heightening quantum mechanical effects that disrupt long range order in the process. A similar mechanism of the enhancement of quantum fluctuations upon doping with N^{3-} is likely to be responsible for the pronounced linear term in the heat capacity of $Lu_2Mo_2O_5N_2$ in comparison to $Lu_2Mo_2O_7$. The low temperature heat capacity of $Lu_2Mo_2O_5N_2$ also provides an upper limit for any gap in the spin excitation spectrum, $\Delta \sim 0.5$ K $\sim$0.05 meV. Neutron spectroscopic data [Figs. 3(b) and 5] set the upper limit for a gap at $\sim$0.1 meV.

We finally turn to the relationship between the ground states of $Lu_2Mo_2O_7$ and $Y_2Mo_2O_7$. The ionic radius of Lu^{3+} is $\sim$4% smaller than that of Y^{3+} [43], yet both oxides are "disorder free" spin glasses with similar T_f. It is intriguing that a second pyrochlore antiferromagnet with a single magnetic site displays such similar behavior. If weak disorder is responsible for this state, it would imply that this disorder is very similar in the two materials, which is not obvious based on their ionic radii. Short range spin correlations within these two spin glass ground states are similar but distinct. $Y_2Mo_2O_7$ [17] displays a broad elastic magnetic peak centered at 0.4 Å^{-1}, as compared with the peak at 0.6 Å^{-1} reported here for $Lu_2Mo_2O_7$. The lower Q position of the peak of $Y_2Mo_2O_7$ indicates that its magnetic correlations have a longer ranged spatial extent. Indeed, those in $Y_2Mo_2O_7$ were found to form domains extending over an entire unit cell, whereas those in $Lu_2Mo_2O_7$ are confined to a next-nearest-neighbor length scale, roughly half a unit cell.

To conclude, the unconventional spin glass state observed in $Lu_2Mo_2O_7$ is similar to that shown by $Y_2Mo_2O_7$, but with shorter range static correlations peaked at $Q = 0.6$ Å^{-1}. In contrast to the oxide, $Lu_2Mo_2O_5N_2$ shows no evidence for any transition to a frozen or ordered state to 0.5 K. The strength of the quantum fluctuations induced by the the reduction of S in the oxynitride overcomes any competition with disorder in the selection of a ground state and gives rise to a QSL, with an upper bound on a gap in the spin excitation spectrum of $\Delta \sim 0.05$ meV $\sim$0.5 K or $\Delta/|\theta| \sim 0.004$. This study demonstrates the potential of nitriding oxide precursors as a means of tuning the oxidation state on magnetic ions, and therefore the spin degree of freedom and strength of quantum fluctuations.

This is a relatively unexplored route to exotic magnetic ground states, but one with the potential to be very rewarding.

Work at McMaster University was supported by NSERC. Work at the University of Edinburgh was supported by EPSRC and STFC. Research at Oak Ridge National Laboratory's Spallation Neutron Source was supported by the Scientific User Facilities Division, Office of Basic Energy Sciences, U.S. Department of Energy. L. C. gratefully acknowledges useful discussions with J. R. Stewart, C. Stock, and M. A. de Vries and support from the University of Edinburgh.

[1] J. E. Greedan, J. Mater. Chem. **11**, 37 (2001).
[2] P. W. Anderson, Mater. Res. Bull. **8**, 153 (1973).
[3] L. Balents, Nature (London) **464**, 199 (2010).
[4] P. Mendels, F. Bert, M. A. de Vries, A. Olariu, A. Harrison, F. Duc, J. C. Trombe, J. S. Lord, A. Amato, and C. Baines, Phys. Rev. Lett. **98**, 077204 (2007).
[5] M. A. de Vries, J. R. Stewart, P. P. Deen, J. O. Piatek, G. J. Nilsen, H. M. Rønnow, and A. Harrison, Phys. Rev. Lett. **103**, 237201 (2009).
[6] B. Fåk, E. Kermarrec, L. Messio, B. Bernu, C. Lhuillier, F. Bert, P. Mendels, B. Koteswararao, F. Bouquet, J. Ollivier, A. D. Hillier, A. Amato, R. H. Colman, and A. S. Wills, Phys. Rev. Lett. **109**, 037208 (2012).
[7] L. Clark, J. C. Orain, F. Bert, M. A. de Vries, F. H. Aidoudi, R. E. Morris, P. Lightfoot, J. S. Lord, M. T. F. Telling, P. Bonville, J. P. Attfield, P. Mendels, and A. Harrison, Phys. Rev. Lett. **110**, 207208 (2013).
[8] M. Yamashita, N. Nakata, Y. Senshu, M. Nagata, H. M. Yamamoto, R. Kato, T. Shibauchi, and Y. Matsuda, Science **328**, 1246 (2010).
[9] K. A. Ross, L. Savary, B. D. Gaulin, and L. Balents, Phys. Rev. X **1**, 021002 (2011).
[10] B. Canals and C. Lacroix, Phys. Rev. Lett. **80**, 2933 (1998).
[11] E. Berg, E. Altman, and A. Auerbach, Phys. Rev. Lett. **90**, 147204 (2003).
[12] M. Hermele, M. P. A. Fisher, and L. Balents, Phys. Rev. B **69**, 064404 (2004).
[13] A. Harrison, J. Phys. Condens. Matter **16**, S553 (2004).
[14] N. Hanasaki, K. Watanabe, T. Ohtsuka, I. Kézsmárki, S. Iguchi, S. Miyasaka, and Y. Tokura, Phys. Rev. Lett. **99**, 086401 (2007).
[15] J. E. Greedan, M. Sato, X. Yan, and F. S. Razavi, Solid State Commun. **59**, 895 (1986).
[16] M. J. P. Gingras, C. V. Stager, N. P. Raju, B. D. Gaulin, and J. E. Greedan, Phys. Rev. Lett. **78**, 947 (1997).
[17] J. S. Gardner, B. D. Gaulin, S.-H. Lee, C. Broholm, N. P. Raju, and J. E. Greedan, Phys. Rev. Lett. **83**, 211 (1999).
[18] K. Miyoshi, Y. Nishimura, K. Honda, K. Fujiwara, and J. Takeuchi, J. Phys. Soc. Jpn. **69**, 3517 (2000).
[19] H. J. Silverstein, K. Fritsch, F. Flicker, A. M. Hallas, J. S. Gardner, Y. Qiu, G. Ehlers, A. T. Savici, Z. Yamani, K. A. Ross, B. D. Gaulin, M. J. P. Gingras, J. A. M. Paddison, K. Foyevtsova, R. Valenti, F. Hawthorne, C. R. Wiebe, and H. D. Zhou, Phys. Rev. B **89**, 054433 (2014).
[20] L. Clark, C. Ritter, A. Harrison, and J. P. Attfield, J. Solid State Chem. **203**, 199 (2013).
[21] M. Yang, J. Oró-Solé, A. Fuertes, and J. P. Attfield, Chem. Mater. **22**, 4132 (2010).
[22] See the Supplemental Material at http://link.aps.org/supplemental/10.1103/PhysRevLett.113.117201, including Refs. [23–27], for further experimental details regarding sample synthesis, susceptibility, and neutron scattering measurements.
[23] A. C. Larson and R. B. Von Dreele, Los Alamos National Laboratory Report No. LAUR 86-748 (1994).
[24] V. F. Sears, Neutron News **3**, 26 (1992).
[25] D. Schmitt and B. Ouladdiaf, J. Appl. Crystallogr. **31**, 620 (1998).
[26] C. W. Dwiggins, Acta Crystallogr. Sect. A **31**, 146 (1975).
[27] R. T. Azuah, L. R. Kneller, Y. Qiu, P. L. W. Tregenna-Piggott, C. M. Brown, J. R. D. Copley, and R. M. Dimeo, J. Res. Natl. Inst. Stand. Technol. **114**, 341 (2009).
[28] J. R. Stewart, P. P. Deen, K. H. Andersen, H. Schober, J. F. Barthélémy, J. M. Hillier, A. P. Murani, T. Hayes, and B. Lindenau, J. Appl. Crystallogr. **42**, 69 (2009).
[29] O. Schärpf and H. Capellmann, Phys. Status Solidi A **135**, 359 (1993).
[30] G. Ehlers, J. R. Stewart, A. R. Wildes, P. P. Deen, and K. H. Andersen, Rev. Sci. Instrum. **84**, 093901 (2013).
[31] G. J. Nilsen, F. C. Coomer, M. A. de Vries, J. R. Stewart, P. P. Deen, A. Harrison, and H. M. Rønnow, Phys. Rev. B **84**, 172401 (2011).
[32] P. J. Brown, *International Tables for Crystallography* (Kluwer Academic, London, 2004).
[33] A. S. Wills, G. S. Oakley, D. Visser, J. Frunzke, A. Harrison, and K. H. Andersen, Phys. Rev. B **64**, 094436 (2001).
[34] R. Cywinski, S. Kilcoyne, and J. R. Stewart, Physica (Amsterdam) **267B**, 106 (1999).
[35] G. Ehlers, A. A. Podlesnyak, J. L. Niedziela, E. B. Iverson, and P. E. Sokol, Rev. Sci. Instrum. **82**, 085108 (2011).
[36] H. Shinaoka, Y. Motome, T. Miyake, and S. Ishibashi, Phys. Rev. B **88**, 174422 (2013).
[37] M. A. de Vries, K. V. Kamenev, W. A. Kockelmann, J. Sanchez-Benitez, and A. Harrison, Phys. Rev. Lett. **100**, 157205 (2008).
[38] S. Yamashita, Y. Nakazawa, M. Oguni, Y. Oshima, H. Nojiri, Y. Shimizu, K. Miyagawa, and K. Kanoda, Nat. Phys. **4**, 459 (2008).
[39] V. Y. Irkhin and M. I. Katsnelson, Pis'ma Zh. Eksp. Teor. Fiz. **49**, 500 (1989) [JETP Lett. **49**, 576 (1989)].
[40] O. Nakamura, A. Oyamada, A. Ochiai, S. Kunii, T. Takeda, T. Suzuki, and T. Kasuya, J. Magn. Magn. Mater. **76–77**, 293 (1988).
[41] H. Wada, H. Nakamura, E. Fukami, K. Yoshimura, M. Shiga, and Y. Nakamura, J. Magn. Magn. Mater. **70**, 17 (1987).
[42] V. Y. Irkhin and M. I. Katsnelson, Phys. Lett. A **150**, 47 (1990).
[43] R. D. Shannon, Acta Crystallogr. Sect. A **32**, 751 (1976).